Eur. Phys. J. C 46, s02, 21–31 (2006)
Digital Object Identifier (DOI) 10.1140/epjcd/s2006-03-003-5

EPJ C direct
electronic only

Young Scientist

Searches for new physics in photon final states

A. Loginov[a]

SSC RF ITEP, Bolshaya Cheremushkinskaya, 25, 117218 Moscow, Russia

Received: 30 June 2006 /
Published online: 28 July 2006 –

Abstract. The Run I results on the searches for new physics in photon final states were intriguing. The rare $ee\gamma\gamma\not{E}_{\mathrm{T}}$ candidate event and the measured event rate for the signature $\ell+\gamma+\not{E}_{\mathrm{T}}$, which was 2.7 sigma above the Standard Model predictions, sparked signature-based searches in the $\gamma\gamma+X$ and $\ell\gamma+X$ channels. With more data in Run II we should be able to answer a simple question: was it an anomaly or were the Run I results the first evidence for new physics? We present searches for new physics in photon final states at CDF Run II, Fermilab, with substantially more data and a higher $\bar{p}p$ collision energy, 1.96 TeV, and the upgraded CDF-II detector.

PACS. 13.85.Rm; 12.60.Jv; 13.85.Qk; 14.80.Ly; 14.80.-j

1 Introduction

The Standard Model (sm) [1] is an effective field theory that has so far described the fundamental interactions of elementary particles remarkably well. However the model breaks down at energies of a few TeV, in that the cross-section for scattering of longitudinal W bosons would otherwise violate unitarity. The Fermilab Tevatron has the highest center-of-mass energy collisions of any present accelerator, with $\sqrt{s} = 1.96\,\mathrm{TeV}$, and thus has the potential to discover new physics. As of September, 2005, the CDF experiment at Fermilab has recorded $1\,\mathrm{fb}^{-1}$ of data. Physics results using $202\,\mathrm{pb}^{-1}$ to $345\,\mathrm{pb}^{-1}$ are presented in this paper.

1.1 Motivation

Why do we consider the photon final states a good signature for observing new physics?

- well motivated theories
  - Most importantly supersymmetry
- History
  - Follow up on some of the anomalies from CDF in Run I [2–6]
- From the experimentalists' point of view, just because...
  - The photon is coupled to electric charge, and thus is radiated by all charged particles, including the incoming states (important for searching for invisible final states)
  - The photon is massless and thus kinematically easier to produce than the W or Z
  - The photon is stable, which implies a high acceptance, as there are no branching ratios to 'pay'
  - The photon is a boson and could be produced by a fermiphobic parent
  - And if we then require
    - Additional lepton(s) $\Rightarrow$ high-$\mathrm{E_T}$[1] photon + high-$\mathrm{P_T}$ lepton + X signature is rare in sm, backgrounds are low for searches
    - Additional photon(s) $\Rightarrow$ the photons have moderate signal-to-noise but good efficiency and mass peak resolution

1.2 Run I results

1.2.1 $ee\gamma\gamma\not{E}_{\mathrm{T}}$ candidate event

In 1995 the CDF experiment, measuring $\bar{p}p$ collisions at a center-of-mass energy of 1.8 TeV at the Fermilab Tevatron, observed an event [2, 3, 7] consistent with the produc-

[a] e-mail: loginov@fnal.gov
For the CDF Collaboration

[1] Transverse momentum and energy are defined as $\mathrm{P_T} = p\sin\theta$ and $\mathrm{E_T} = E\sin\theta$, respectively. The CDF coordinate system of r, φ, and z is cylindrical, with the z-axis along the proton beam. The pseudorapidity is $\eta = -\ln(\tan(\theta/2))$.

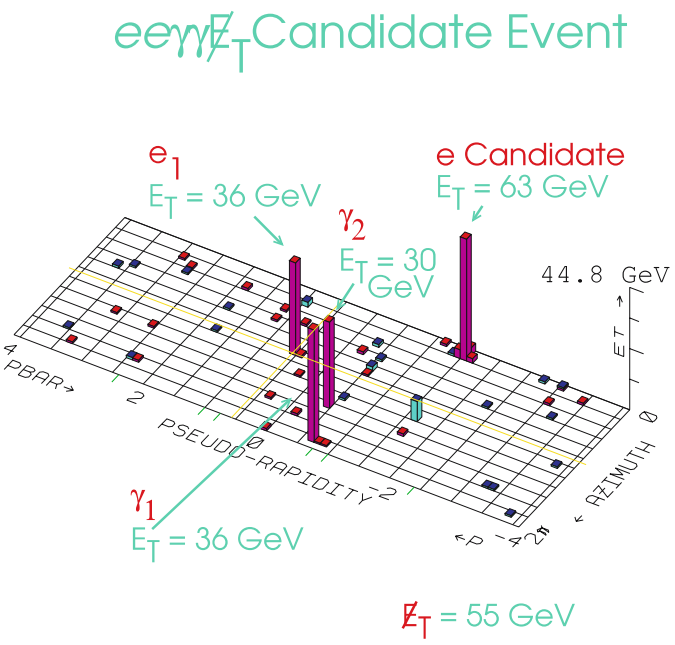

Fig. 1. The Run I $ee\gamma\gamma\not\!\!E_{\rm T}$ candidate event

tion of two energetic photons, two energetic electrons, and large missing transverse energy[2], $\not\!\!E_{\rm T}$ (Fig. 1).

This signature is predicted to be very rare in the Standard Model of particle physics, with the dominant contribution coming from the $WW\gamma\gamma$ production:

$$WW\gamma\gamma \to (e\nu)(e\nu)\gamma\gamma \to ee\gamma\gamma\not\!\!E_{\rm T}\,,$$

from which we expect 8×10^{-7} events. All other sources (mostly detector misidentification) lead to 5×10^{-7} events. Therefore, we expect $(1\pm1)\times10^{-6}$ events, which would give us one $ee\gamma\gamma\not\!\!E_{\rm T}$ candidate event if we had taken million times more data than we actually had in Run I.

The event raised theoretical interest, however, as the two-lepton two-photon signature is expected in some models of physics 'beyond the Standard Model' such as gauge-mediated models of supersymmetry [8]. For example, possible interpretation will be:

$$p\overline{p} \to \tilde{\rm e}^+\tilde{\rm e}^-(+X)\,, \tilde{\rm e} \to \tilde{\chi}_2^0 + {\rm e}\,, \tilde{\chi}_2^0 \to \tilde{\chi}_1^0\gamma\,,$$

where $\tilde{e}$ is the selectron (the bosonic partner of the electron), and $\tilde{\chi}_1^0$ and $\tilde{\chi}_2^0$ are the lightest and next-to-lightest neutralinos.

1.2.2 $\gamma\gamma+$X Search

The detection of this single event led to the development of 'signature-based' inclusive searches to cast a wider net: in this case one searches for two photons $+X$ [2, 3, 7], where X stands for anything, with the idea that if pairs of new particles were being created these inclusive signatures would be sensitive to a range of decay modes or to the creation and decay of different particle types.

In Run I Searches for $\gamma\gamma+X$ all results were consistent with the sm background expectations with no other exceptions other than the observation of the $ee\gamma\gamma\not\!\!E_{\rm T}$ candidate event (Table 1) [3].

[2] Missing E_T ($\not\!\!E_T$) is defined by $\not\!\!E_{\rm T} = -\sum_i E_{\rm T}^i \hat{n}_i$, where i is the calorimeter tower number for $|\eta| < 3.6$, and $\hat{n}_i$ is a unit vector perpendicular to the beam axis and pointing at the i^{th} calorimeter tower. We define the magnitude $\not\!\!E_{\rm T} = |\not\!\!E_{\rm T}|$.

Table 1. Number of observed and expected $\gamma\gamma$ events with additional objects in 86 pb^{-1} [3]

Signature (Object)	Obs.	Expected
$\not\!\!E_{\rm T}c > 35$ GeV, $\lvert\Delta\phi_{\not\!\!E_{\rm T}-\rm jet}\rvert > 10^\circ$	1	0.5 ± 0.1
$N_{\rm jet} \geq 4$, $E_{\rm T}^{\rm jet} > 10$ GeV, $\lvert\eta^{\rm jet}\rvert < 2.0$	2	1.6 ± 0.4
b-tag, $E_{\rm T}^b > 25$ GeV	2	1.3 ± 0.7
Central γ, $E_{\rm T}^{\gamma_3} > 25$ GeV	0	0.1 ± 0.1
Central e or μ, $E_{\rm T}^{e\ \rm or\ \mu} > 25$ GeV	3	0.3 ± 0.1
Central τ, $E_{\rm T}^{\tau} > 25$ GeV	1	0.2 ± 0.1

Table 2. Run I Photon-Lepton Results: Number of observed and expected $\ell\gamma$ events with additional objects in 86 pb^{-1} [6]

Category	$\mu_{\rm SM}$	N_0	$P(N \geq N_0\lvert\mu_{\rm SM})$,%
All $\ell\gamma+X$	–	**77**	–
Z-like $e\gamma$	–	17	–
Two-Body $\ell\gamma X$	24.9±2.4	33	9.3
Multi-Body $\ell\gamma X$	20.2±1.7	27	10.0
Multi-Body $\ell\ell\gamma X$	5.8 ± 0.6	5	68.0
Multi-Body $\ell\gamma\gamma X$	0.02±0.02	1	1.5
Multi-Body $\ell\gamma\not\!\!E_{\rm T}X$	**7.6** ± 0.7	**16**	**0.7**

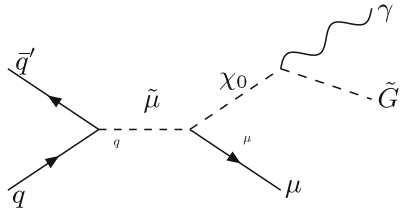

Fig. 2. Resonant smuon production and subsequent decay, producing the $\mu\gamma\not\!\!E_{\rm T}$ signature

In Run I Searches for $\gamma\gamma+X$ all results were consistent with the sm background expectations with no other exceptions other than the observation of the $ee\gamma\gamma\not\!\!E_{\rm T}$ candidate event (Table 1) [3].

1.2.3 From $\gamma\gamma$ to $\ell\gamma$: $\ell\gamma+X$ Search

Another 'signature-based' inclusive search, motivated by $ee\gamma\gamma\not\!\!E_{\rm T}$ event was for $\ell\gamma+X$ [5, 6, 9].

In general data agrees with expectations, with the exception for the $\ell\gamma\not\!\!E_{\rm T}$ category (Table 2). We have observed 16 $\ell\gamma\not\!\!E_{\rm T}$ events on a background of 7.6 ± 0.7 expected. The 16 $\ell\gamma\not\!\!E_{\rm T}$ events consist of 11 $\mu\gamma\not\!\!E_{\rm T}$ events and 5 $e\gamma\not\!\!E_{\rm T}$ events, versus expectations of 4.2 ± 0.5 and 3.4 ± 0.3 events, respectively. The sm prediction yields the observed rate of $\ell\gamma\not\!\!E_{\rm T}$ with 0.7% probability (which is equivalent to 2.7 standard deviations for a Gaussian distribution).

One of the first SUSY interpretation of the CDF $\mu\gamma\not\!\!E_{\rm T}$ events [10] was resonant smuon $\tilde{\mu}$ production with a single dominant R-parity violating coupling (Fig. 2).

The Run I search was initiated by an anomaly in the data itself, and as such the 2.7 sigma excess above the sm expectations must be viewed taking into account the number of such channels a fluctuation could have occurred in.

2 From Run I to Run II

Having many different hints from the signature-based searches for new physics in photon final states in Run I, the strategy for Run II was straightforward: take more data. The main points were:

- Increase the collision energy: $1.80 \to 1.96$ TeV
- Increase the rate at which we take data: $3500 \to 396$ ns (timing between bunches)
- Upgrade the detectors

2.1 CDF Run II detector

The CDF-II detector [11] is a cylindrically symmetric spectrometer designed to study $\bar{p}p$ collisions at the Fermilab Tevatron, that uses the same solenoidal magnet and central calorimeters as the CDF-I detector [12] from which it was upgraded. Because the analyses described here have been motivated by the Run I searches, we note especially the differences from the Run I detector relevant to the detection of photons, leptons, and $\not\!\!E_{\rm T}$.

The central calorimeters are physically unchanged; however, the readout electronics has been replaced to accommodate the smaller proton and anti-proton bunch spacing of the Tevatron in Run II. The end-cap (plug) and forward calorimeters have been replaced with a more compact scintillator-based design, retaining the projective geometry [13].

The tracking system used to measure the momenta of charged particles has been replaced, with the central outer tracker upgraded to have smaller drift cells [14], and the inner tracking chamber and silicon system replaced by a system of silicon strip chambers with more layers, now in 2-dimensions [15]. The new inner tracking system has substantially more material, resulting in more bremsstrahlung (photons) produced by high-$\rm P_T$ electrons.

The central CMU, CMP, and CMX muon systems[3] are also physically unchanged in design, but the coverage of the CMP and CMX muon systems [16] has been extended by filling in gaps in φ [11].

3 Run II: searches for new physics in photon final states

The Run I results on the searches for new physics in photon final states were intriguing [2, 3, 5, 6]. The rare $ee\gamma\gamma\not\!\!E_{\rm T}$ candidate event and the measured event rate for the signature $\ell + \gamma + \not\!\!E_{\rm T}$, which was 2.7 sigma above the sm predictions, sparked signature-based searches in the $\gamma\gamma + X$ and $\ell\gamma + X$ channels.

With more data in Run II we should be able to answer a simple question: was it an anomaly or were the Run I results the first evidence for the new physics?

There are lots of searches involving photon final states at CDF in Run II. Some of the analyses are presented in this paper:

- Search for high-mass diphoton state and limits on randall–sundrum gravitons (Sect. 3.1)
- Search for anomalous production of diphoton events with $\not\!\!E_{\rm T}$ and limits on GMSB models (Sect. 3.2)
- Search for lepton–photon–X events (Sect. 3.3)

3.1 Search for high-mass diphoton state and limits on Randall–Sundrum gravitons

Searches for new particles decaying into two identical particles are broad, inclusive and sensitive. The production of the new particle may be direct or in association with other particles, or in a decay chain. The discovery of a sharp mass peak over background would be a compelling evidence for the production of a new particle. The diphoton final state is important because the photons are bosons and the parent may be fermiphobic. The photons have moderate signal-to-noise but good efficiency and mass peak resolution.

One model producing a diphoton mass peak is Randall–Sundrum gravitons [17]. Current string theory proposes that as many as seven new dimensions may exist and the geometry of these extra dimensions is responsible for gravity being so weak. The Randall–Sundrum model has the property that a parameter, the warp factor, determines the curvature of the extra dimensions and therefore the mass of the Kaluza–Klein graviton resonances, which decay to two bodies including photons.

Details on this analysis are reported in [18].

3.1.1 Data sample

The sample corresponds to $345\ \rm pb^{-1}$ of data taken between February 2002 and July 2004. We require that the data were taken under good detector conditions for a reliable photon identification. We apply selection cuts as follows:

- Photons in central calorimeter
- $\rm E_T^{\gamma} > 15$ GeV
- $\rm M(\gamma, \gamma) > 30$ GeV

To select a photon in a central calorimeter (approximately $0.05 < |\eta| < 1.0$), we require a central electromagnetic cluster that: a) is not near the boundary in ϕ of a calorimeter tower[4]; b) have the ratio of hadronic to electromagnetic energy, Had/EM, $< 0.055 + 0.00045 \times E^{\gamma}(\rm GeV)$; c) have no track track with $\rm P_T > 1\ GeV/c$, and at most one track with $\rm P_T < 1$ GeV, pointing at the clus-

[3] The CMU (Central Muon Chambers) system consists of gas proportional chambers in the region $|\eta| < 0.6$; the CMP (Central Muon Upgrade) system consists of chambers after an additional meter of steel, also for $|\eta| < 0.6$. The CMX (Central Muon Extension) chambers cover $0.6 < |\eta| < 1.0$.

[4] The fiducial region has $\sim 87\%$ coverage in the central region.

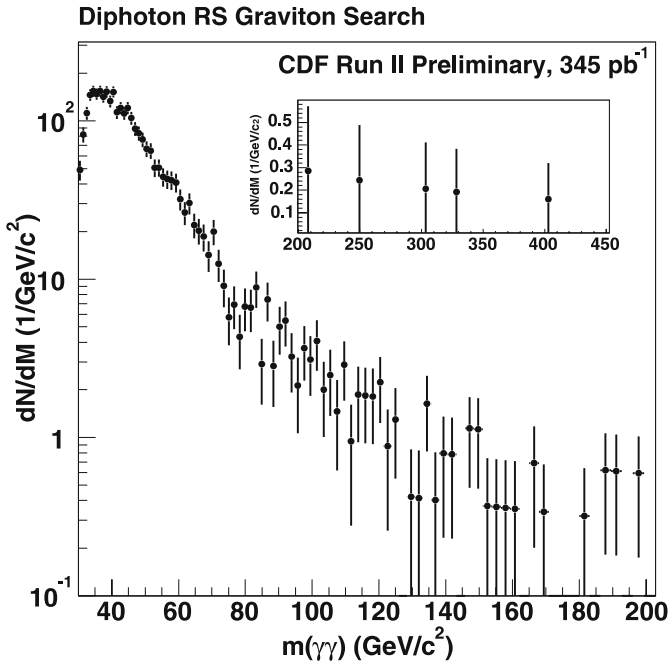

Fig. 3. The diphoton invariant mass distribution histogrammed in bins of approximately one σ of mass resolution

ter; d) is isolated in the calorimeter and tracking chamber[5]; e) have a shower shape in the CES[6] consistent with a single photon; f) have no other significant energy deposited nearby in the CES.

The final dataset consists of 3339 events, for which the data histogrammed with bins equivalent to one σ of invariant mass resolution are shown in Fig. 3. The highest mass events occur at masses of 207, 247, 304, 329, and 405 GeV/c^2 (Fig. 4).

3.1.2 Backgrounds

There are two significant backgrounds to the $\gamma\gamma$ sample. The first is sm diphoton production which accounts for 30% of the events (Fig. 5). This background is estimated using a NLO Monte Carlo, diphox [19], which we normalize to $\mathcal{L} = 345\,\mathrm{pb}^{-1}$.

The second background comes from high-E_T π^0's from jets. To create a control sample, we loosen several cuts (including relaxing the isolation cuts by 50%), and we get 9891 events, from which we then reject events in the sig-

[5] To reject hadronic backgrounds that fake prompt photons, candidates are required to be isolated in the calorimeter and tracking chamber. In the calorimeter the isolation is defined as the energy in a cone of 0.4 in $\eta - \phi$ space, minus the photon cluster energy, and corrected for energy loss into cracks as well as the number of reconstructed $\bar{p}p$ interactions in the event. We require isolation $< 0.1 \times E_T^\gamma$ for $E_T^\gamma < 20$ GeV, and < 2.0 GeV $+ 0.02 \times (E_T^\gamma - 20$ GeV) for $E_T^\gamma > 20$ GeV. In the tracking chamber we require the scalar sum of the P_T of all tracks in a cone of 0.4 to be < 2.0 GeV $+ 0.005 \times E_T^\gamma$, where all values of E_T^γ are in GeV.

[6] CES: Central EM Strip Chambers.

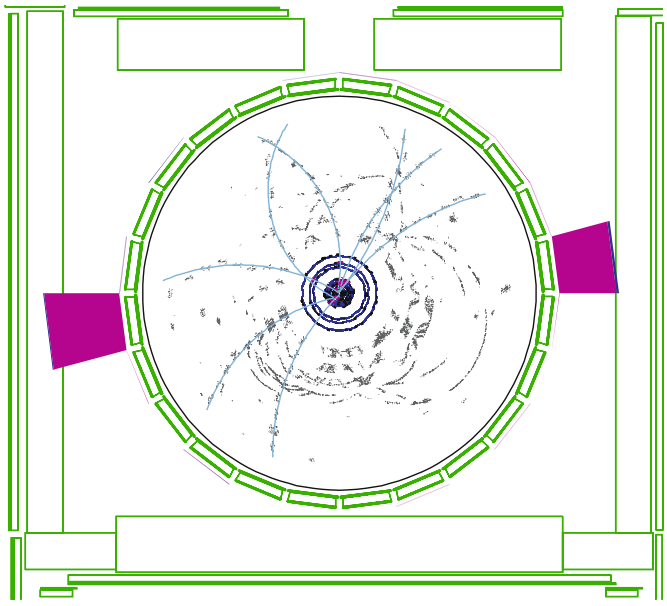

Fig. 4. $\gamma\gamma$ highest mass event. $M(\gamma\gamma) = 405$ GeV/c^2, $E_T^{\gamma 1} = 172$ GeV, $E_T^{\gamma 2} = 175$ GeV

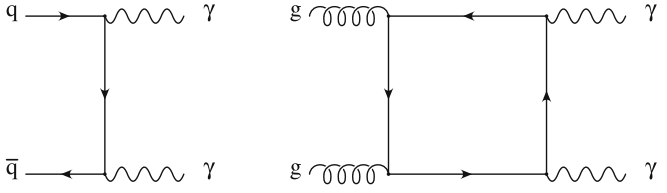

Fig. 5. Standard Model diphoton production diagrams

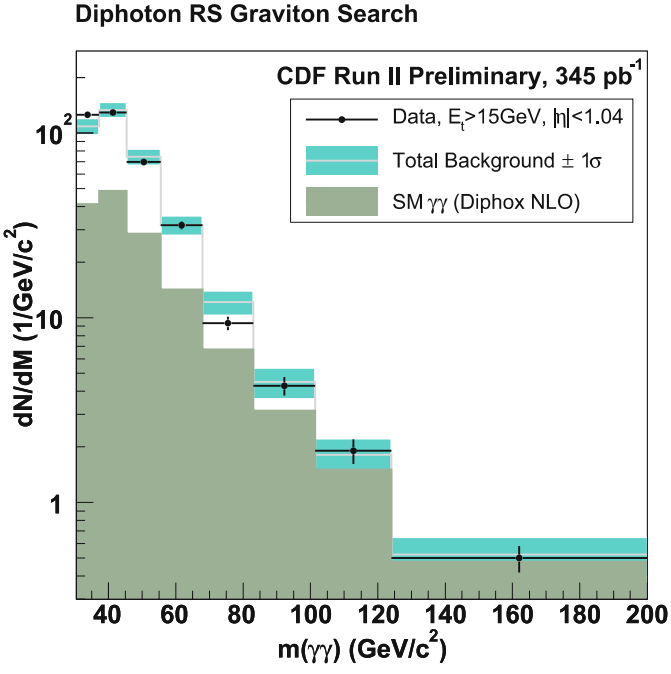

Fig. 6. Comparison of the sm di-photon contribution plus misidentified jets with the observed diphoton mass spectrum. Variable bins are used for statistical comparison to the background prediction

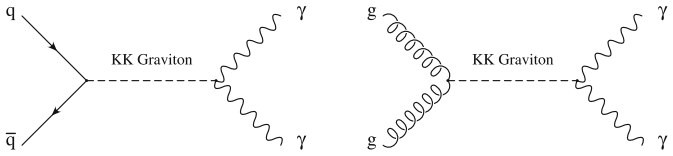

Fig. 7. Randall–Sundrum graviton production and decay to diphotons

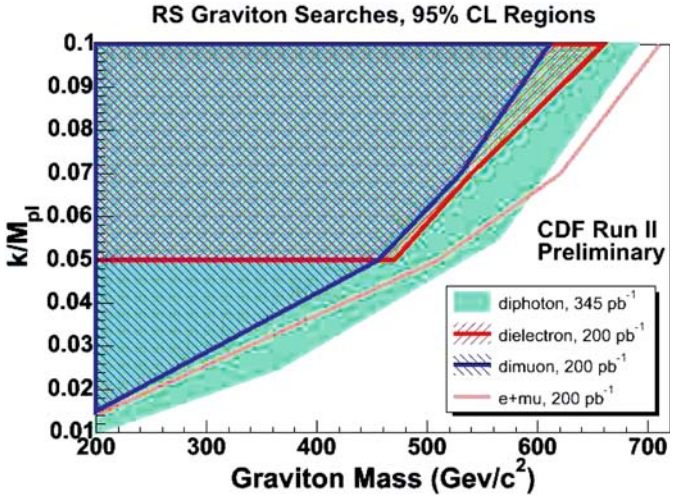

Fig. 8. Combined 95% confidence level Randall–Sundrum graviton mass limits of the di-photon and di-lepton searches

nal sample and are left with 6552 events in the "photon sideband" sample. We then derive the shape of the mass distribution by fitting this sample to a sum of several exponentials. We then subtract the estimate from the sm contribution and normalize the fakes background to the low mass ($m_{\gamma\gamma}$ between 30 and 100 GeV).

Figure 6 shows the data mass spectrum compared to the prediction.

3.1.3 Limits on Randall–Sundrum gravitons

Since the data are consistent with the sm prediction, we place upper limits on the cross sections times branching ratio of Randall–Sundrum graviton production and decay to diphotons (Fig. 7).

Figure 8 shows the combined 95% confidence level RS graviton mass limits of the di-photon ($\mathcal{L} = 345\,\mathrm{pb}^{-1}$) and di-lepton ($\mathcal{L} = 200\,\mathrm{pb}^{-1}$) searches [20] in the graviton mass versus coupling, k/M_{Planck}, plane. Note, that $\gamma\gamma$ has a larger Branching Ratio ($\mathrm{Br}(\mathrm{G} \to \gamma\gamma) = 2 \times \mathrm{Br}(\mathrm{G} \to \mathrm{ee})$) and the $\gamma\gamma$ spin factors improve the acceptance.

3.2 Search for anomalous production of diphoton events with $\not\!\!E_{\mathrm{T}}$ and limits on GMSB models

For theoretical reasons [21, 22], and because of the $ee\gamma\gamma\not\!\!E_{\mathrm{T}}$ candidate event (Fig. 1) recorded by the CDF detector in Run I [2, 3], we want to search for the production of heavy new particles that decay producing the signature $\gamma\gamma + \not\!\!E_{\mathrm{T}}$. Of particular theoretical interest are supersymmetric (SUSY) models with gauge-mediated SUSY-breaking (GMSB). Characteristically, the effective SUSY-breaking scale (Λ) can be as low as 100 TeV, the lightest SUSY particle is a light gravitino ($\tilde{G}$) that is assumed to be stable, and the SUSY particles have masses in a range that may make them accessible at Tevatron energies [21]. In these models the visible signatures are determined by the properties of the next-to-lightest SUSY particle (NLSP) that may be, for example, a slepton or the lightest neutralino ($\tilde{\chi}_1^0$). In the GMSB model investigated here, the NLSP is a $\tilde{\chi}_1^0$ decaying almost exclusively to a photon and a $\tilde{G}$ that penetrates the detector without interacting, producing $\not\!\!E_{\mathrm{T}}$. SUSY particle production at the Tevatron is predicted to be dominated by pairs of the lightest chargino ($\tilde{\chi}_1^{\pm}$) and by associated production of a $\tilde{\chi}_1^{\pm}$ and the next-to-lightest neutralino ($\tilde{\chi}_2^0$). Each gaugino pair cascades down to two $\tilde{\chi}_1^0$'s, leading to a final state of $\gamma\gamma + \not\!\!E_{\mathrm{T}} + X$, where X represents any other final state particles.

Details on this analysis can be found in [23, 24].

3.2.1 Data sample

The analysis selection criteria have been optimized to maximize, *a priori*, the expected sensitivity to GMSB SUSY based only on the background expectations and the predictions of the model. Event selection requirements for the diphoton candidate sample are designed to reduce electron and jet/π^0 backgrounds while accepting well-measured diphoton candidates.

We require two central (approximately $0.05 < |\eta| < 1.0$) electromagnetic clusters that should pass standard photon selection cuts (Sect. 3.1.1). For this analysis we require $\mathrm{E}_{\mathrm{T}}^{\gamma} > 13$ GeV.

3.2.2 Backgrounds

Backgrounds for the $\gamma\gamma + X$ analysis are:

- QCD background: fake photon ($jj, j\gamma$)
- QCD background: $\gamma\gamma$
- $e\gamma$
- Non-collision: beam-related, cosmic rays

Before the $\not\!\!E_{\mathrm{T}}$ requirement, the diphoton candidate sample is dominated by QCD interactions producing combinations of photons and jets faking photons. In each case only small measured $\not\!\!E_{\mathrm{T}}$ is expected, due mostly to energy measurement resolution effects.

Events with an electron and a photon candidate ($W\gamma \to e\nu\gamma$, $Wj \to e\nu\gamma_{\mathrm{fake}}$, $Z\gamma \to ee\gamma$, etc.) can contribute to the diphoton candidate sample when the electron track is lost (by tracking inefficiency or bremsstrahlung) to create a fake photon. For W decays large $\not\!\!E_{\mathrm{T}}$ can come from the neutrinos. This background is estimated using $e\gamma$ events from the data.

Beam-related sources and cosmic rays overlapped with a sm event can contribute to the background by producing spurious energy deposits that in turn affect the measured $\not\!\!E_{\mathrm{T}}$. While the rate at which these events contribute to the diphoton candidate sample is low, most contain large $\not\!\!E_{\mathrm{T}}$. The spurious clusters can pass photon cuts.

Table 3. Numbers of events observed and events expected from background sources as a function of the $\not\!\!E_T$requirement. Here "QCD" includes the $\gamma\gamma$, γj and jj processes. The first uncertainty is statistical, the second is systematic

$\not\!\!E_T$	Expected				Observed
Requirement	QCD	$e\gamma$	Non-collision	Total	
25 GeV	$4.01 \pm 3.21 \pm 3.76$	$1.40 \pm 0.52 \pm 0.45$	$0.54 \pm 0.06 \pm 0.42$	$5.95 \pm 3.25 \pm 3.81$	3
35 GeV	$0.30 \pm 0.24 \pm 0.22$	$0.84 \pm 0.32 \pm 0.27$	$0.25 \pm 0.04 \pm 0.19$	$1.39 \pm 0.40 \pm 0.40$	2
45 GeV	$0.01 \pm 0.01 \pm 0.01$	$0.14 \pm 0.06 \pm 0.05$	$0.12 \pm 0.03 \pm 0.09$	$0.27 \pm 0.07 \pm 0.10$	0
55 GeV	(negligible)	$0.05 \pm 0.03 \pm 0.02$	$0.07 \pm 0.02 \pm 0.05$	$0.12 \pm 0.04 \pm 0.05$	0

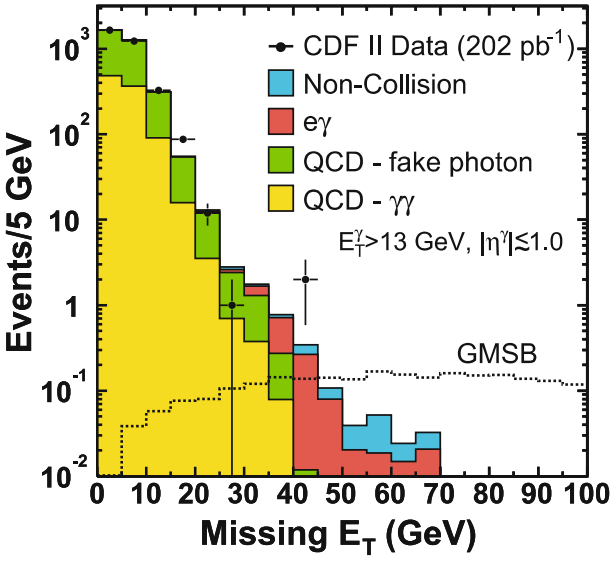

Fig. 9. The $\not\!\!E_T$ spectrum for events with two isolated central photons with $E_T^\gamma > 13$ GeV and $|\eta| \lesssim 1.0$ along with the predictions from the GMSB model with a $\tilde{\chi}_1^\pm$ mass of 175 GeV/c^2, normalized to 202 pb^{-1}. The diphoton candidate sample data are in good agreement with the background predictions. There are no events above the $\not\!\!E_T > 45$ GeV threshold. The properties of the two candidates above 40 GeV appear consistent with the expected backgrounds

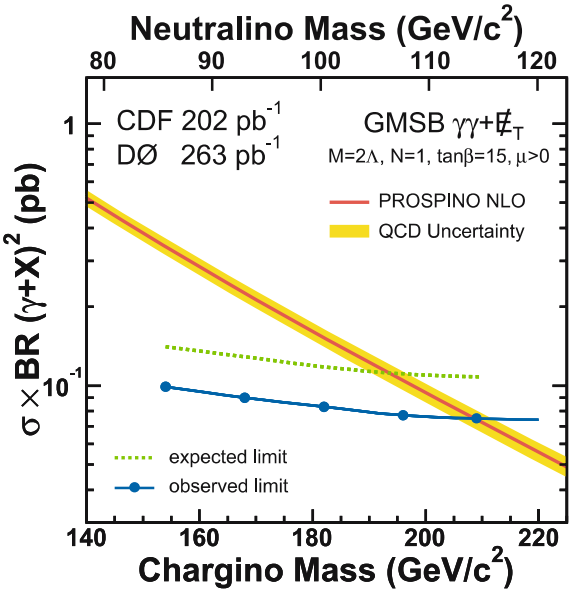

Fig. 10. The 95% C.L. upper limits on the total production cross section times branching ratio versus $M_{\tilde{\chi}_1^\pm}$ and $M_{\tilde{\chi}_1^0}$ for the light gravitino scenario using the parameters proposed in [25]. The lines show the experimental combined CDF + DØ limit and the LO and NLO theoretically predicted cross sections. We set limits of $M_{\tilde{\chi}_1^\pm} > 209$ GeV/c^2, $M_{\tilde{\chi}_1^0} > 114$ GeV/c^2, $\Lambda > 84.6$ GeV/c^2 at 95% C.L. in GMSB Model

Backgrounds and observed number of events are summarized in Table 3.

3.2.3 Limits on GMSB models

The $\not\!\!E_T$ spectrum for events with two isolated central photons with $E_T^\gamma > 13$ GeV is shown in Fig. 9, along with the predictions from the GMSB model. No excess is observed in two photons + energy imbalance events.

Since there is no evidence for events with anomalous $\not\!\!E_T$ in the diphoton candidate sample, we set limits on new particle production from GMSB using the parameters suggested in [25]. Using the NLO predictions we set a limit of $M_{\tilde{\chi}_1^\pm}$, and then from mass relations in the model, we equivalently set limits on $M_{\tilde{\chi}_1^0}$ and Λ:

$$M_{\tilde{\chi}_1^\pm} > 167\ \text{GeV/c}^2\,, M_{\tilde{\chi}_1^0} > 93\ \text{GeV/c}^2\,, \Lambda > 69\ \text{GeV/c}^2\,.$$

The combined CDF + DØ limit [24] is significantly larger (i.e. more stringent) than either experiment alone [23, 26]. The details on the combination of the results on the CDF and DØ searches for chargino and neutralino production in GMSB SUSY using the two-photon and missing E_T channel are explained in [24].

Figure 10 shows the combined CDF and DØ result for the observed cross section [24] as a function of $M_{\tilde{\chi}_1^\pm}$ and $M_{\tilde{\chi}_1^0}$ along with the theoretical LO and NLO production cross sections.

The combined CDF + DØ limits are:

$$M_{\tilde{\chi}_1^\pm} > 209\ \text{GeV/c}^2\,, M_{\tilde{\chi}_1^0} > 114\ \text{GeV/c}^2\,, \Lambda > 84.6\ \text{GeV/c}^2$$

at 95% C.L. in GMSB Model. This is a first combined Run II result and it sets the world's most stringent limits on the GMSB SUSY.

3.3 Search for lepton–photon–X events

In Run I lepton + photon + X search the results were consistent with sm expectations in a number of channels with "the possible exception of photon–lepton events with large $\not\!\!E_T$, for which the observed total was 16 events and the sm expectation was 7.6 ± 0.7 events, corresponding in likelihood to a 2.7 sigma effect." [6]). We concluded "However, an excess of events with 0.7% likelihood (equivalent to 2.7 standard deviations for a Gaussian distribution) in one subsample among the five studied is an interesting result, but it is not a compelling observation of new physics. We look forward to more data in the upcoming Run of the Fermilab Tevatron." [6]. In this section we report the results [27] of repeating the $\ell\gamma + X$ search with the same kinematic selection criteria in a substantially larger data set, $\mathcal{L} = 305\,\mathrm{pb}^{-1}$, a higher $\bar{p}p$ collision energy, 1.96 TeV, and the CDF II detector.

3.3.1 Data sample

The data presented here were taken between March 21, 2002, and August 22, 2004 and represent $305\,\mathrm{pb}^{-1}$ for which the silicon detector and all three central muon systems (CMP, CMU and CMX) were operational.

A 3-level trigger [11] system selects events with a high transverse momentum[7] lepton ($\mathrm{P_T} > 18\,\mathrm{GeV}$) or photon ($\mathrm{E_T} > 25\,\mathrm{GeV}$) in the central region, $|\eta| \lesssim 1.0$. Photon and electron candidates are chosen from clusters of energy in adjacent CEM[8] towers; electrons are then further separated from photons by requiring the presence of a COT[9] track pointing at the cluster. Muons are identified by requiring COT tracks to extrapolate to a reconstructed track segment in the muon drift chambers.

We have reused the Run I selection kinematic cuts for Run II analysis, so that they are *a priori*:

- *Tight* muons: $\mathrm{P_T} > 25$ GeV
- *Tight* central electrons, photons: $\mathrm{E_T} > 25$ GeV
- *Loose* muons: $\mathrm{P_T} > 20$ GeV
- *Loose* central electrons: $\mathrm{E_T} > 20$ GeV
- *Loose* plug electrons: $\mathrm{E_T} > 15$ GeV
- $\not\!\!E_T > 25$ GeV

The identification of photons (see Sect. 3.1.1) and leptons is essentially the same as in the Run I search [5], with only minor technical differences, mostly due to the changes in the construction of the tracking system and end-plug calorimeters.

A muon passing the 'tight' cuts is required to: a) have a track in the COT that passes quality cuts on the minimum number of hits on the track; b) deposit energy in the electromagnetic and hadronic compartments of the calorimeter consistent with that expected from a muon, c) match a muon 'stub' track in the CMX detector or in both the CMU and CMP detectors; d) not be a cosmic ray (determined from measuring timing with the COT).

'Tight' central electrons are required to have a high-quality track with $\mathrm{P_T}$ of at least half the shower energy[10], minimal leakage into the hadronic calorimeter[11], a good profile in the z dimension (the dimension in which the electron track is not bent by the magnetic field) at shower maximum that matches the extrapolated track position, and a lateral sharing of energy in the two calorimeter towers containing the electron shower consistent with that expected.

The additional muons are required to have $\mathrm{P_T} > 20$ GeV and to satisfy the same criteria as for "tight" muons but with fewer hits required on the track, or, alternatively, a more stringent cut on track quality but no requirement that there be a matching "stub" in the muon systems. Additional central electrons are required to have $\mathrm{E_T} > 20$ GeV and to satisfy the tight central electron criteria but with a track requirement of only $\mathrm{P_T} > 10$ GeV (rather than $0.5 \times \mathrm{E_T}$), and no requirement on a shower maximum measurement or lateral energy sharing between calorimeter towers. 'Loose' electrons in the end-plug calorimeters are required to have $\mathrm{E_T} > 15\,\mathrm{GeV}$, minimal leakage into the hadron calorimeters, a 'track' containing at least 3 hits in the silicon tracking system, and a shower transverse shape consistent with that expected, with a centroid close to the extrapolated position of the track.

Missing transverse energy $\not\!\!E_T$ is calculated from the calorimeter tower energies in the region $|\eta| < 3.6$. Corrections are then made to the $\not\!\!E_T$ for non-uniform calorimeter response [28] for jets with uncorrected $\mathrm{E_T} > 15\,\mathrm{GeV}$ and $\eta < 2.0$, and for muons with $\mathrm{P_T} > 20$ GeV.

3.3.2 Control samples and backgrounds

We use W and Z^0 production as control samples to ensure that the efficiencies for high-$\mathrm{P_T}$ electrons and muons, as well as for $\not\!\!E_T$, are well understood. The photon control sample is constructed from events in which one of the electrons radiates a high-$\mathrm{E_T}$ γ such that the $e\gamma$ invariant mass is within 10 GeV of the Z^0 mass.

The dominant source of photon-lepton events at the Tevatron is electroweak diboson production (Fig. 11), in which a W or Z^0 boson decays leptonically ($\ell\nu$ or $\ell\ell$) and a photon is radiated from either an initial-state quark, the W or Z^0, or from a charged final-state lepton. The number of such events is estimated using leading-order (LO) matrix element event generators [30–32]. A correction for higher-order processes (K-factor) has been applied [29].

To simulate the triboson channels $W\gamma\gamma$ and $Z\gamma\gamma$ we have used MadGraph [30] and CompHep[32].

3.3.3 Lepton–photon–X results

Following the Run I analysis strategy, we define the $\ell\gamma\not\!\!E_T$ subsample by requiring that an event contains, in addition

[7] We use the convention that "momentum" refers to pc and "mass" to mc^2.

[8] CEM: Central EM Calorimeter.

[9] COT: Central Outer Tracker.

[10] The $\mathrm{P_T}$ threshold is set to 25 GeV for $\mathrm{E_T} > 100$ GeV.

[11] The fraction of electromagnetic energy E_{em} allowed to leak into the hadronic compartment is $0.055 + 0.00045 E_{\mathrm{em}}$ for tight and loose central electrons; for loose plug electrons and for photons the fraction must be less than 0.125.

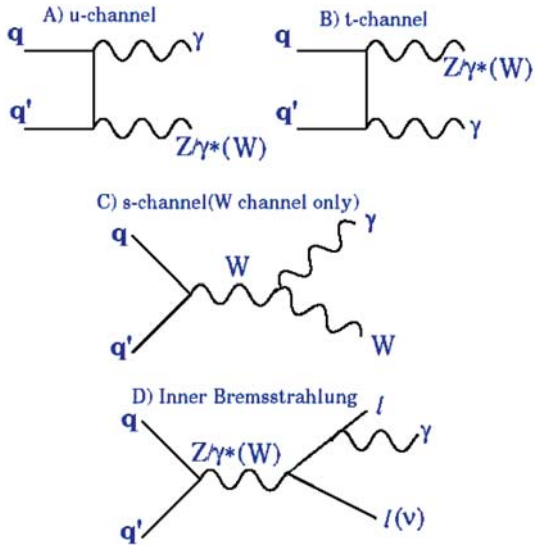

Fig. 11. Standard Model $W\gamma$ and $Z\gamma$ production diagrams

to the central lepton and central photon, $\not\!\!E_T > 25$ GeV. A second signal subsample, the $\ell\ell\gamma$ sample, is constructed by requiring, in addition to the central lepton and central photon, a second 'loose' lepton with $E_T > 25$ GeV. These two subsamples were selected as the search regions of interest from the Run I results with the same kinematic selections; these two searches in the Run II data are thus *a priori*. Both sample selections are 'inclusive', in that there are no requirements on the presence or absence of other objects.

In addition to the expectations from real sm processes that produce real lepton–photon events, there are backgrounds due to misidentified leptons and photons, and also incorrectly calculated $\not\!\!E_T$.

We consider two sources of fake photons: QCD jets in which a π^0 or a photon from hadron decay mimics a direct photon, and electron bremsstrahlung, in which an energetic photon is radiated off of an electron which then has much lower energy and curls away from the photon.

Backgrounds from fake leptons and/or fake missing E_T ('QCD') we estimate from a sample, in which we expect to have very little real lepton content [33] by selecting on loose leptons and rejecting events from the W or Z.

The predicted and observed totals for both the $\ell\gamma\not\!\!E_T$ and $\ell\ell\gamma$ searches are shown in Table 4. We observe 42 $\ell\gamma\not\!\!E_T$

Table 4. A comparison of the numbers of events predicted by the sm and the observations for the $\ell\gamma\not\!\!E_T$ and $\ell\ell\gamma$ searches. The sm predictions are dominated by $W\gamma$ and $Z\gamma$ production [30–32]. Other contributions come from $W\gamma\gamma$ and $Z\gamma\gamma$, leptonic τ decays, and misidentified leptons, photons, or $\not\!\!E_T$

	Lepton + photon + $\not\!\!E_T$ events		
SM source	$e\gamma\not\!\!E_T$	$\mu\gamma\not\!\!E_T$	$(e+\mu)\gamma\not\!\!E_T$
$W^{\pm}\gamma$	13.70±1.89	8.84±1.35	22.54±2.80
$Z^0/\gamma^* + \gamma$	1.16±0.40	4.49±0.64	5.65±1.03
$W^{\pm}\gamma\gamma, Z^0/\gamma^* + \gamma\gamma$	0.14±0.02	0.18±0.02	0.32±0.03
$W^{\pm}\gamma, Z^0/\gamma^* + \gamma \to \tau\gamma$	0.71±0.18	0.26±0.08	0.97±0.22
$W^{\pm}$ + Jet fakingγ	2.8±2.8	1.6±1.6	4.4±4.4
$Z^0/\gamma^* \to e^+e^-, e \to \gamma$	2.45±0.33	–	2.45±0.33
Jets faking$\ell + \not\!\!E_T$	0.7±0.7	0.3±0.3	1.0±0.8
Total	**21.7±3.4**	**15.7±2.2**	**37.3±5.4**
Observed	**25**	**17**	**42**
	Multi-lepton + photon events		
SM Source	$ee\gamma$	$\mu\mu\gamma$	$ll\gamma$
$Z^0/\gamma^* + \gamma$	12.50±1.53	7.81±0.88	20.31±2.40
$Z^0/\gamma^* + \gamma\gamma$	0.24±0.03	0.12±0.02	0.36±0.04
Z^0/γ^* + Jet fakingγ	0.3±0.3	0.2±0.2	0.5±0.5
$Z^0/\gamma^* \to e^+e^-, e \to \gamma$	0.23±0.09	–	0.23±0.09
Jets faking$\ell + \not\!\!E_T$	0.6±0.6	1.0±1.0	1.6±1.2
Total	**13.9±1.7**	**9.1±1.4**	**23.0±2.7**
Observed	**19**	**12**	**31**

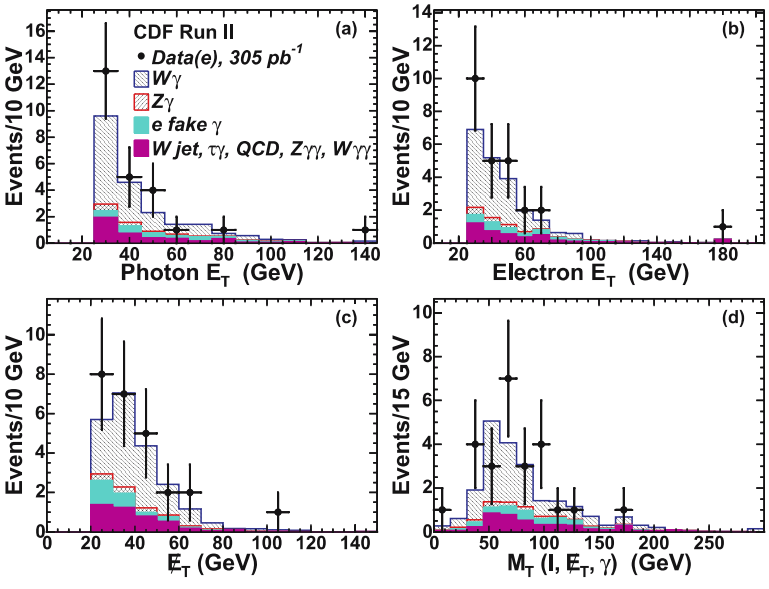

Fig. 12. The distributions for events in the $e\gamma\not\!\!E_T$ sample in **a** the E_T of the photon; **b** the E_T of the electron, **c** the missing transverse energy, $\not\!\!E_T$, and **d** the transverse mass of the electron–photon–$\not\!\!E_T$ system. The histograms show the expected sm contributions, including estimated backgrounds from misidentified photons and leptons

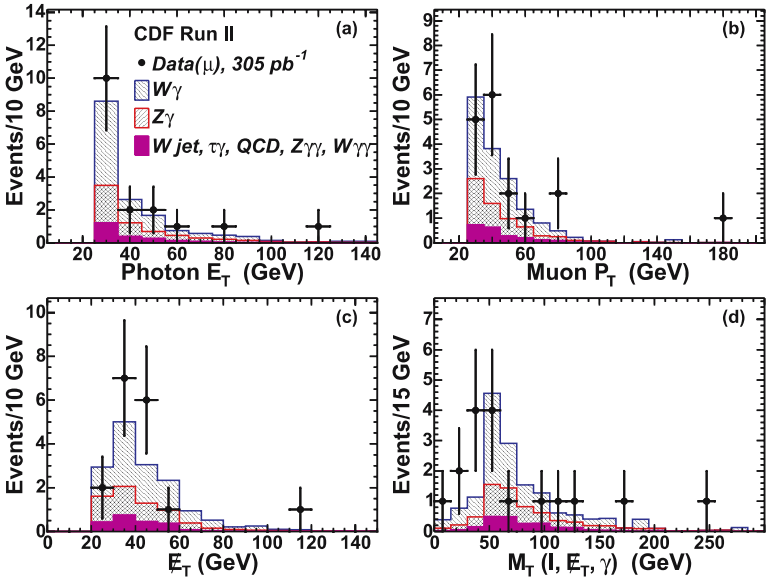

Fig. 13. The distributions for events in the $\mu\gamma\not\!\!E_{\rm T}$ sample in **a** the E_T of the photon; **b** the P_T of the muon, **c** the missing transverse energy, $\not\!\!E_{\rm T}$, and **d** the transverse mass of the muon–photon-$\not\!\!E_{\rm T}$ system. The histograms show the expected sm contributions, including estimated backgrounds from misidentified photons and leptons

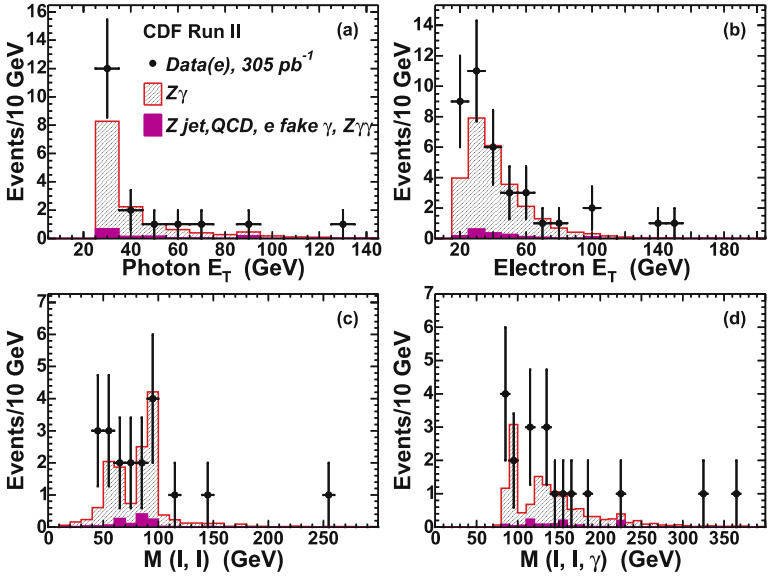

Fig. 14. The distributions in **a** the E_T of the photon; **b** the E_T of the electron, **c** the 2-body mass of the dielectron system, and **d** the 3-body invariant mass $m_{ee\gamma}$

events, versus the expectation of 37.3 ± 5.4 events. If the Run I ratio of observed to expected, which was 16/7.6, had held up, the $2.7\,\sigma$ excess observed in Run I would have resulted in an observation of 79 ± 11 events when applying the same analysis to the Run II data, versus the 42 events observed. In the $\ell\ell\gamma$ channel, we observe 31 events, versus an expectation of 23.0 ± 2.7 events. No $e\mu\gamma$ events are observed.

While the number of events observed is somewhat larger than expectations (Table 4), there is not a significant excess in either signature, and the kinematic distributions are in reasonable agreement with the sm predicted shapes.

The distributions for events in the $\ell\gamma\not\!\!E_{\rm T}$ sample are shown in Fig. 12 for the electron channel and in Fig. 13 for the muon channel. The dominant contribution for $\ell\gamma\not\!\!E_{\rm T}$ is sm $Z\gamma$ and $W\gamma$ production.

The distributions for events in the $\ell\ell\gamma$ sample are shown at Fig. 14 for electron channel and Fig. 15 for muon channel. The dominant contribution for $\ell\ell\gamma$ is sm $Z\gamma$ production.

For the $Z\gamma$ process occurring via initial state radiation, the dilepton invariant mass distribution will be peaked around the Z^0-pole. For the final state radiation, the three body invariant mass ($m(l, l, \gamma)$) distribution will be peaked around the Z^0-pole (Figs. 14, 15c and d).

We do not expect missing E_T in the events in the $\ell\ell\gamma$ sample based on the sm backgrounds; the $ee\gamma\gamma\not\!\!E_{\rm T}$ event was of special interest due to the large value of $\not\!\!E_{\rm T}$. Figure 16 shows the distributions in $\not\!\!E_{\rm T}$ for the $ee\gamma$ and $\mu\mu\gamma$ subsamples of the $\ell\ell\gamma$ sample. No events are observed with $\not\!\!E_{\rm T} > 25$ GeV.

In conclusion, we have repeated the search for inclusive lepton + photon production with the same kinematic requirements as the Run I search, but with a significantly larger data sample and a higher collision energy. We find

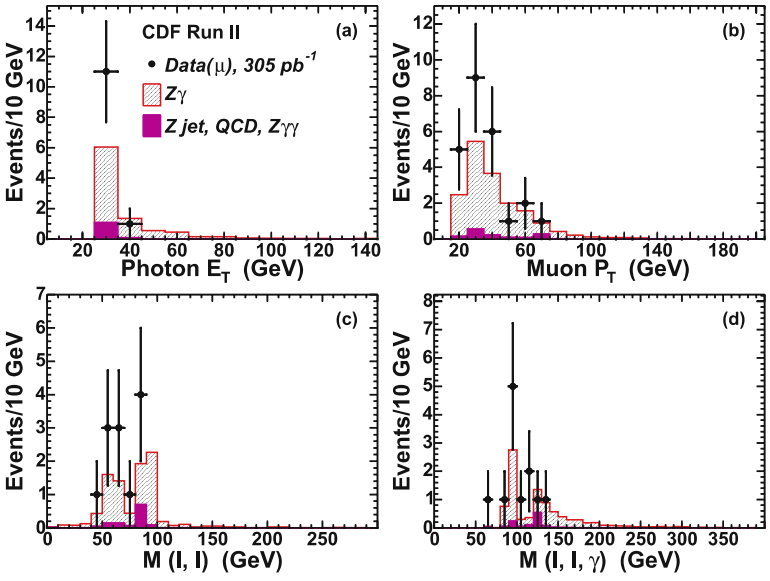

Fig. 15. The distributions in **a** the E_T of the photon; **b** the P_T of the muon, **c** the 2-body mass of the dimuon system, and **d** the 3-body invariant mass $m_{\mu\mu\gamma}$

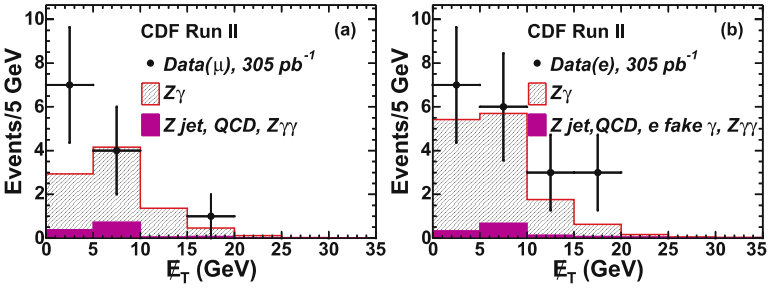

Fig. 16. The distributions in missing transverse energy $\not\!\!E_T$ observed in the inclusive search for **a** $\mu\mu\gamma$ events and **b** $ee\gamma$ events. The histograms show the expected sm contributions

that the numbers of events in the $\ell\gamma\not\!\!E_T$ and $\ell\ell\gamma$ subsamples of the $\ell\gamma + X$ sample agree with sm predictions. We observe no $\ell\ell\gamma$ events with anomalous large $\not\!\!E_T$ or with multiple photons and so find no events like the $ee\gamma\gamma\not\!\!E_T$ event of Run I.

In summary, while we are disappointed that we found no more $ee\gamma\gamma\not\!\!E_T$ events in a much larger sample than in Run I, and the Run I excess in $\ell\gamma\not\!\!E_T$ became less significant rather than more, we have conclusively settled a question that generated much interest in the theoretical community. The channels we have investigated will remain interesting, and the techniques we have developed and the knowledge gained will be useful for similar searches at the Tevatron and at the LHC.

4 Summary and outlook

To summarize, we will list the main points for the Run II results presented in this paper:

- Search for $\ell\gamma + X$: the Run I 2.7 sigma excess in $\ell\gamma\not\!\!E_T$ is not confirmed when repeating the analysis with much more data. We observe no $\ell\ell\gamma$ events with anomalous large $\not\!\!E_T$ or with multiple photons.
- Search for $\gamma\gamma\not\!\!E_T + X$: no excess is observed in the two photons + energy imbalance channel. The combined CDF and DØ Result provides world's most stringent limits on GMSB SUSY. No new $ee\gamma\gamma\not\!\!E_T$ (or similar) candidate events have been found.
- Search for high-mass diphotons: the data agree with predictions.

The Fermilab plan is to have a factor of 10–20 more data than presented here by the end of Run II of the Tevatron. A recent upgrade, the EM Timing system [34], provides a vitally important handle that could confirm (or disprove) that all the photons in unusual events are from the primary collision.

Currently, the CDF is actively pursuing topics and analyzing up to 1 fb^{-1} of delivered luminosity. New and exciting results are coming out quickly. Further information regarding the analyses presented in this paper and new results can be found in [35].

References

1. S.L. Glashow, Nucl. Phys. **22**, 588 (1961); S. Weinberg, Phys. Rev. Lett. **19**, 1264 (1967); A. Salam, Proc. 8th Nobel Symposium, Stockholm, 1979
2. F. Abe et al., Phys. Rev. D **59**, 092002 (1999) [hep-ex/9806034]
3. F. Abe et al., Phys. Rev. Lett **81**, 1791 (1998) [hep-ex/9801019]

4. D. Affolder et al., Phys. Rev. D **65**, 052 006 (2002) [hep-ex/0106012]
5. D. Acosta et al., Phys. Rev. D **66**, 012 004 (2002) [hep-ex/0110015]
6. D. Acosta et al., Phys. Rev. Lett **89**, 041 802 (2002) [hep-ex/0202004]
7. D. Toback, Ph.D. thesis, University of Chicago, 1997
8. S. Ambrosanio, G.L. Kane, G.D. Kribs, S.P. Martin, S. Mrenna, Phys. Rev. D **55**, 1372 (1997); B.C. Allanach, S. Lola, K. Sridhar, Phys. Rev. Lett. **89**, 011 801 (2002) [hep-ph/0111014]
9. J. Berryhill, Ph.D. thesis, University of Chicago, 2000
10. B.C. Allanach, S. Lola, K. Sridhar, Phys. Rev. Lett. **89**, 011 801 (2002) [hep-ph/0111014]
11. CDF Collaboration, D. Acosta et al., Phys. Rev. D **71**, 032 001 (2005)
12. F. Abe et al., Nucl. Instrum. Methods Phys. Res. A **271**, 387 (1988)
13. S. Kuhlmann et al., Nucl. Instrum. Methods A **518**, 39 (2004)
14. T. Affolder et al., Nucl. Instrum. Methods A **526**, 249 (2004)
15. A. Sill et al. Nucl. Instrum. Methods A **447**, 1 (2000); T. Affolder et al., Nucl. Instrum. Methods A **453**, 84 (2000); C.S. Hill, Nucl. Instrum. Methods A **530**, 1 (2000)
16. CDF Collaboration, R. Blai et al., FERMILAB-PUB-96/390-E (1996), Chapter 10
17. L. Randall, R. Sundrum, Phys. Rev. Lett **83**, 3370 (1999) [hep-ph/9905221]
18. CDF Collaboration, D. Acosta et al., http://www-cdf.fnal.gov/physics/exotic/r2a/20040805.diphoton_rsgrav
19. See wwwlapp.in2p3.fr/lapth/PHOX_FAMILY/readme_diphox.html
20. High Mass Dielectrons: http://fcdfhome.fnal.gov/usr/ikado/Bless_Fall_2003/Bless_fall2003.html; High Mass Dimuons: http://www-cdf.fnal.gov/physics/exotic/run2/highmass-mumu-2004/blessed_plots_win04.html
21. S. Dimopoulos, S. Thomas, J.D. Wells, Nucl. Phys. B **488**, 39 (1997); S. Ambrosanio, G.D. Kribs, S.P. Martin, Phys. Rev. D **56**, 1761 (1997); G.F. Giudice, R. Rattazzi, Phys. Rept. **322**, 419 (1999); S. Ambrosanio, G.L. Kane, G.D. Kribs, S.P. Martin, S. Mrenna, Phys. Rev. D **55**, 1372 (1997)
22. R. Culbertson et al., hep-ph/0008070
23. CDF Collaboration, D. Acosta et al., Phys. Rev. D **71**, 031 104 (2005) [hep-ex/0410053]
24. CDF and DØ Collaborations, V. Buescher, R. Culbertson et al., hep/ex 0504004
25. B.C. Allanach et al., Eur. Phys. J. C **25**, 113 (2002) We take the messenger mass scale $M_M = 2\Lambda$, $\tan(\beta) = 15$, $\mathrm{sign}(\mu) = 1$, the number of messenger fields $N_M = 1$, and negligibly short $\tilde{\chi}_1^0$ lifetimes.
26. DØ Collaboration, V.M. Abazov et al., Phys. Rev. Lett. **94**, 041 801 (2005) [hep-ex/0408146]
27. CDF Collaboration, A. Abulencia et al., Phys. Rev. Lett **97**, 031 801 (2006); hep-ex/0605097
28. A. Bhatti et al., accepted to Nucl. Instrum. Methods A (2006); hep-ex/0510047
29. U. Baur, T. Han, J. Ohnemus, Phys. Rev. D **48**, 5140 (1993); U. Baur, T. Han, J. Ohnemus, Phys. Rev. D **57**, 2823 (1998) [hep-ph/9710416]; Both the $W\gamma$ and $Z\gamma$ K-factors are fixed at 1.36 for generated $\ell\nu$ masses below 76 GeV and for generated $\ell^+\ell^-$ masses below 86 GeV. Above the poles the K-factors grow with E_T^γ to be 1.62 and 1.53 at $E_T^\gamma = 100$ GeV for $W\gamma$ and $Z\gamma$, respectively.
30. T. Stelzer, W.F. Long, Comput. Phys. Commun. **81**, 357 (1994); F. Maltoni, T. Stelzer, JHEP **0302**, 027 (2003) [hep-ph/0208156]
31. U. Baur, T. Han, J. Ohnemus, Phys. Rev. D **57**, 2823 (1998) [hep-ph/9710416]; U. Baur, T. Han, J. Ohnemus, Phys. Rev. D **48**, 5140 (1993) [hep-ph/9305314]
32. E. Boos et al., INP-MSU-98-41-542, hep-ph/9908288; E. Boos et al., INP MSU 94-36/358 and SNUTP-94-116, hep-ph/9503280
33. S. Kopp, Ph.D. thesis, University of Chicago, 1994
34. "The Timing System for the CDF Electromagnetic Calorimeters", M. Goncharov et al., to be submitted to NIM
35. See http://www-cdf.fnal.gov/physics/exotic/exotic.html